



ChemComm

**Chalcogen-Atom Abstraction Reactions of a Di-Iron
Imidophosphorane Complex**

Journal:	<i>ChemComm</i>
Manuscript ID	CC-COM-04-2021-002195.R2
Article Type:	Communication

SCHOLARONE™
Manuscripts

COMMUNICATION

Chalcogen-Atom Abstraction Reactions of a Di-Iron Imidophosphorane Complex

Received 00th January 20xx,
Accepted 00th January 20xx

Luis M. Aguirre Quintana,^a Yan Yang,^b Arun Ramanathan,^a Ningxin Jiang,^a John Bacsa,^a Laurent Maron,^b and Henry S. La Pierre^{*a,c}

DOI: 10.1039/x0xx00000x

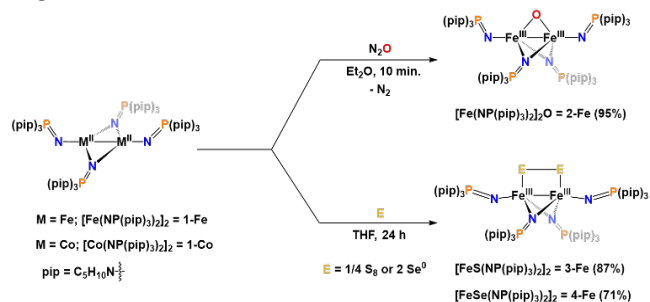
Reaction of the complexes $[\text{Fe}_2(\mu_2\text{-NP}(\text{pip})_3)_2(\text{NP}(\text{pip})_3)_2]$ (1-Fe) and $[\text{Co}_2(\mu_2\text{-NP}(\text{pip})_3)_2(\text{NP}(\text{pip})_3)_2]$ (1-Co), where $[\text{NP}(\text{pip})_3]^{1-}$ is tris(piperidinyl)imidophosphorane, with nitrous oxide, S_8 , or Se^0 result in divergent reactivity. With nitrous oxide, 1-Fe forms $[\text{Fe}_2(\mu_2\text{-O})(\mu_2\text{-NP}(\text{pip})_3)_2(\text{NP}(\text{pip})_3)_2]$ (2-Fe), with a very short $\text{Fe}^{3+}\text{-Fe}^{3+}$ distance. Reactions of 1-Fe with S_8 or Se^0 results in the bridging, side-on coordination ($\mu\text{-}\kappa^1\text{:}\kappa^1\text{-E}_2^{2-}$) of the heavy chalcogens in complexes $[\text{Fe}_2(\mu\text{-}\kappa^1\text{:}\kappa^1\text{-E}_2)(\mu_2\text{-NP}(\text{pip})_3)_2(\text{NP}(\text{pip})_3)_2]$ (E = S, 3-Fe, or Se, 4-Fe). In all cases, the complex 1-Co is inert.

Molecular metal-metal bonded compounds are a lodestone guiding the understanding of inorganic bonding, reactivity, and magnetism.¹⁻⁴ Recently Berry, Lu, Thomas, and others have demonstrated the cooperative reactivity of bimetallic complexes in the formation of terminal metal-ligand multiple bonds via oxidative atom-transfer reactions.⁵⁻¹¹ In the case of iron and cobalt, most of the compounds with metal-metal bonds, beyond those supported by carbonyl ligands, form paddlewheel clusters with sterically congested ligands that inhibit any cooperative, side-on (or “facial”) reactivity of the metal-metal bond. This limits the scope of atom-transfer reactions that can be accessed with diiron and dicobalt compounds. Recent examples of facial atom-transfer chemistry have been achieved with constrained geometry, strong-field, redox-active ligands.^{12, 13}

An alternative approach is to employ monodentate, weak field ligands to construct reactive bimetallic complexes. Our group has recently employed tris(dialkylamido)-imidophosphoranes to expand the redox chemistry of the lanthanides and actinides.¹⁴⁻¹⁸ Unlike its alkyl counterparts, the dialkylamido backbone in this ligand architecture better

supports the zwitterionic character in the P–N moiety of imidophosphoranes, favoring a $\text{P}^+\text{-N}^{2-}$ configuration. The pseudo-imido character results in a basic 1σ , 2π weak-field donor that is isoelectronic in its donor profile to cyclopentadienyls, or the more similar single-atom donor siloxides.^{19, 20} The steric profile and donor properties of this ligand framework support low-coordinate iron and give rise to clusters with metal-metal bonds. To date, few examples exist of homoleptic iron or cobalt imidophosphorane complexes, of which, most are supported by alkyl backbones and no atom-transfer reactivity has been reported.²⁰⁻²³ To this end, we set out to employ one of the tris(dialkyl)imidophosphorane variants to explore the atom-transfer chemistry between well-defined homoleptic Fe(II) and Co(II) complexes and N_2O , S_8 , and Se^0 .

The reaction of two equivalents of FeCl_2 or CoCl_2 with four equivalents of $\text{K}[\text{NP}(\text{pip})_3]$ in THF^{16} results in the isolation of the bimetallic complexes $[\text{Fe}_2(\mu_2\text{-NP}(\text{pip})_3)_2(\text{NP}(\text{pip})_3)_2]$ (**1-Fe**) and $[\text{Co}_2(\mu_2\text{-NP}(\text{pip})_3)_2(\text{NP}(\text{pip})_3)_2]$ (**1-Co**) in 79% and 73% yield, respectively. Complex **1-Fe** crystallizes in the $\text{P}\bar{1}$ space group with two molecules in the asymmetric unit. Single-crystal XRD (SC-XRD) analysis of **1-Fe** reveals the molecular structure shown in Figure 1. The product is a saddled Fe_2^{4+} bimetallic complex with two $\mu\text{-}[\text{NP}(\text{pip})_3]^-$ ligands bridging each Fe^{2+} center and a terminal $[\text{NP}(\text{pip})_3]^-$ ligand at each metal center. The average Fe–Fe distance in **1-Fe** is 2.6141(6) Å, which falls within the range of a metal-metal bond^{24, 25} with a formal-shortness ratio



Scheme 1. Synthesis of **2-Fe**.

^a Department of Chemistry and Biochemistry, Georgia Institute of Technology, Atlanta, Georgia 30332-0400, USA. E-mail: hsl@gatech.edu

^b Laboratoire de Physique et Chimie des Nano-objects, Institut National Des Sciences Appliquées, 31077 Toulouse, Cedex 4, France.

^c Nuclear and Radiological Engineering Program, Georgia Institute of Technology, Atlanta, Georgia 30332-0400, USA.

† Electronic supplementary information (ESI) available: Experimental procedures and crystallographic data (PDF and CIF). CCDC 2077656, 2077657, 2077658, 2077659, and 2078817. For ESI and crystallographic data in CIF or other electronic format see DOI: XXXXXXXXXXXXXXXXXXXX

(FSR) of 1.05. Crystallographically, **1-Co** is isomorphous and isostructural to **1-Fe** (See ESI).

The $[\text{NP}(\text{pip})_3]^-$ ligand supports low-coordinate Fe^{2+} and Co^{2+} compounds with facially exposed metal-metal bonds. The reactivity of these dimetallic complexes was examined with chalcogen-atom transfer reagents: N_2O , S, and Se^0 . Exposure of a solution of **1-Fe** or **1-Co** to an atmosphere of N_2O led to a reaction in 10 minutes for **1-Fe**. The resulting brown product, $[\text{Fe}_2(\mu_2\text{-O})(\mu_2\text{-NP}(\text{pip})_3)_2(\text{NP}(\text{pip})_3)_2]$, (**2-Fe**), was isolated in 95 % yield. Under the same conditions, **1-Co** showed no reactivity with N_2O . The molecular structure of **2-Fe** is shown in Figure 1 and crystallizes in the $\text{P}\bar{1}$ space group. Similar to **1-Fe**, the structure of **2-Fe** reveals a bimetallic complex with two μ - $[\text{NP}(\text{pip})_3]^-$ ligands bridging the Fe^{3+} centers and a terminal $[\text{NP}(\text{pip})_3]^-$ ligand at each metal center. Additionally, the metal centers are bridged by a $\mu\text{-O}^{2-}$ ligand. The average terminal $\text{Fe}\text{-N}_{\text{imido}}$ distance in **2-Fe** is 1.8372(12) Å and the average bridging $\text{Fe}\text{-N}_{\text{imido}}$ distance is 2.0265(2) Å, which shows elongation in $\text{Fe}\text{-N}_{\text{imido}}$ distances in comparison to **1-Fe**. The average terminal and bridging $\text{P}\text{-N}_{\text{imido}}$ distances in **2-Fe** are 1.5395(2) Å and 1.5475(2) Å, respectively, similar to those in **1-Fe**. Notably, the distance between the $\text{Fe}(\text{III})$ centers in **2-Fe** is 2.3396(6) Å, and is one of the shortest $\text{Fe}\text{-Fe}$ distances, which typically involve Fe_2^{2+} , Fe_2^{3+} , Fe_2^{4+} , and Fe_2^{5+} cores.²⁴ There are no other examples of dinuclear complexes with an Fe_2^{6+} core with metal centers within the metric range for an $\text{Fe}^{3+}\text{-Fe}^{3+}$ bond. The $\text{Fe}\text{-Fe}$ distance in **2-Fe** is in fact shorter than that of a reported single bond distance (248 pm),²⁶ giving it a formal shortness ratio (FSR) of 0.94. Whether this distance is the consequence of a metal-metal bond or the geometric constraint of the bridging O^{2-} is under further investigation.

Nitrous oxide is a greenhouse gas and its potential utilization as a green oxidant has become an important technological target.²⁷ It is a thermodynamically potent oxidant, but kinetically poor.²⁷⁻²⁹ To date, few examples of molecular iron and cobalt compounds have been reported to bind or activate N_2O under mild conditions and stable, oxidized complexes are rare.³⁰⁻³³ Therefore, the reactivity between **1-Fe** and N_2O is noteworthy since it produces an isolable oxygen-atom abstraction product that does not undergo further intramolecular reaction with ligand C-H bonds. To gain insight into the observed reactivity, an energy profile for the reaction between **1-Fe** and N_2O was calculated at the DFT level (B3PW91) as shown in Figure 2. The energy profile reveals initial binding of N_2O in the $\kappa_1\text{-O}$ mode to one of the $\text{Fe}(\text{II})$ centers in **1-Fe** (a $\kappa_2\text{-N,O}$ binding event was not found on the intrinsic reaction coordinate). This unsymmetrical coordination is exothermic by 2.1 kcal.mol⁻¹. From this adduct, the system evolves to a N-O bond breaking transition state. The N-O bond breaking is favoured by the nucleophilic assistance of the second iron center ($\text{Fe}\text{-O}$ distance of 1.99 and 2.53 Å). The associated barrier is 4.1 kcal.mol⁻¹ from the adduct (2.0 kcal.mol⁻¹ from the entrance channel), which is much lower than that calculated for other systems.^{34, 35} Following the intrinsic reaction coordinate, it yields complex **2-Fe** whose formation is thermodynamically favoured with the production and release of N_2 gas. This reaction profile indicates that the

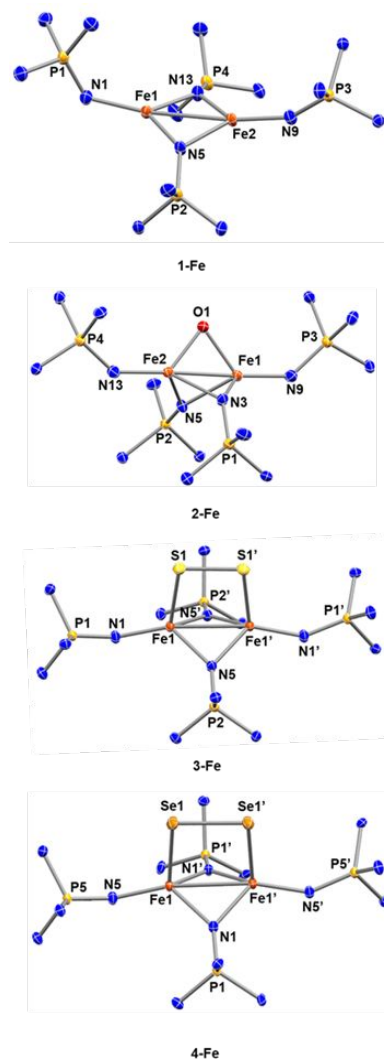


Figure 1. Molecular structures of **1-Fe**, **2-Fe**, **3-Fe**, and **4-Fe** shown with thermal ellipsoids at 50% probability. Piperidinyl carbon and hydrogen atoms are omitted for clarity. Only one of the two molecules in the asymmetric unit of **1-Fe** is shown here. See ESI for full structures.

metal-metal bonded iron centers in **1-Fe** are able to participate synergistically to carry out the two-electron reduction of N_2O by undergoing a one-electron oxidation at each metal center.

To further assess the reactivity of **1-Fe** and **1-Co** with other chalcogen-atom transfer reagents their reactions with elemental sulfur (S_8) and selenium metal powder (Se^0) were examined. In both cases, **1-Fe** or **1-Co** were dissolved in THF and added to a stirring suspension of S_8 or Se^0 . After isolation, $[\text{Fe}_2(\mu\text{-}\kappa^1\text{-}\kappa^1\text{-S}_2)(\mu_2\text{-NP}(\text{pip})_3)_2(\text{NP}(\text{pip})_3)_2]$ (**3-Fe**) and $[\text{Fe}_2(\mu\text{-}\kappa^1\text{-}\kappa^1\text{-Se}_2)(\mu_2\text{-NP}(\text{pip})_3)_2(\text{NP}(\text{pip})_3)_2]$ (**4-Fe**) were recovered in 87 % and 71 %, respectively (Scheme 1). As with the reaction with N_2O , no reaction was observed between **1-Co** and S_8 or Se^0 . Compounds **3-Fe** and **4-Fe** both crystallize in the $\text{C}2/c$ space group and are crystallographic dimers comprised of two μ - $[\text{NP}(\text{pip})_3]^-$ ligands bridging each Fe^{3+} center and a terminal $[\text{NP}(\text{pip})_3]^-$ ligands at each metal center. The metal centers in **3-Fe** and **4-Fe** are bridged by a $(\mu\text{-}\kappa^1\text{-}\kappa^1\text{-S}_2)^{2-}$ and $(\mu\text{-}\kappa^1\text{-}\kappa^1\text{-Se}_2)^{2-}$ ligand, respectively, which sits above and parallel to the to the

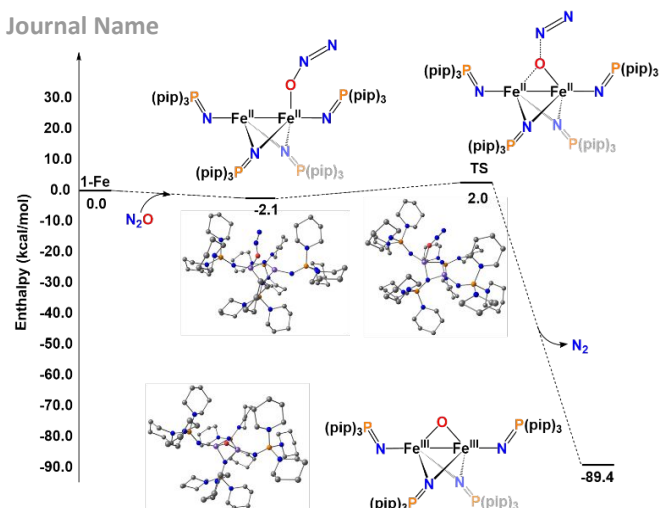


Figure 2. Computed enthalpy profile at room temperature for the reaction of **1-Fe** with N_2O .

Fe–Fe axis in both compounds as shown in Figure 1. The average Fe–E and E–E distances in **3-Fe** and **4-Fe** (where E = S or Se, respectively) are 2.3258(4) and 2.0847(6) Å and 2.4582(8) and 2.3532(8) Å which are consistent with in other reported iron-sulfido and -selenido compounds.^{36–38} The Fe–Fe distances in **3-Fe** and **4-Fe** are 2.5964(6) and 2.6072(6) Å which are longer than **2-Fe**, but have an FSR of 1.05 for both complexes, similar to that of **1-Fe** in the Fe_2^{6+} core.²⁴

The “side-on” binding of the $(\mu\text{-}\kappa^1\text{:}\kappa^1\text{-S}_2)^{2-}$ and $(\mu\text{-}\kappa^1\text{:}\kappa^1\text{-Se}_2)^{2-}$ ligands is unique with E–E bind above and parallel to the Fe–Fe axis in **3-Fe** and **4-Fe**.^{38–41} Iron–sulfido cluster compounds are commonly produced oxidation products from the reduction of elemental sulfur and are bridged by a S^{2-} ligand.⁴² Diiron compounds supported by a S_2^{2-} ligand are rarer and often bridged by a S_2^{2-} that is oblique and/or perpendicular to the Fe–Fe axis.⁴³ Of the few examples of non-carbonyl iron selenido molecular compounds, only one diiron compound presents a similar bridging $(\mu\text{-}\kappa^1\text{:}\kappa^1\text{-Se}_2)^{2-}$ ligand.^{44, 45}

In conclusion, we have reported the synthesis of the homoleptic bimetallic Fe^{2+} and Co^{2+} compounds **1-Fe** and **1-Co** supported by the $[\text{NP}(\text{pip})_3]^-$ ligand, which featured low-coordinate metal-metal bonds with readily accessible synergistic, facial reactivity in the case of **1-Fe**. Compound **1-Fe** displayed unique chalcogen-atom abstraction reactivity with N_2O , S_8 , and Se^0 to produce compounds **2-Fe**, **3-Fe**, **4-Fe**. Structural analysis revealed that **2-Fe** has one of the shortest Fe–Fe distances observed in a diiron compound unsupported by carbonyl or guanidinate ligands and that **3-Fe** and **4-Fe** produce bimetallic compounds with an Fe_2^{6+} core and fairly short intermetallic distances, where the Fe(III) centers are bridged by $(\mu\text{-}\kappa^1\text{:}\kappa^1\text{-S}_2)^{2-}$ and $(\mu\text{-}\kappa^1\text{:}\kappa^1\text{-Se}_2)^{2-}$ ligands parallel to the metal-metal axis. The electronic structure driving the unique and divergent reactivity of **1-Fe** and the structures of **2-Fe**, **3-Fe**, and **4-Fe** will be reported soon.

Conflicts of interest

There are no conflicts to declare.

Acknowledgements

This work was supported by NSF grant CHE-1943452 and a CONACYT Graduate Fellowship to LMAQ. LM is a senior member of the Institut Universitaire de France. The Chinese Scholarship Council and the Chinese Academy of Science are acknowledged for financial support and CalMip for a generous grant of computing time.

References

1. J. F. Berry and C. C. Lu, Metal–Metal Bonds: From Fundamentals to Applications, *Inorg. Chem.*, 2017, **56**, 7577–7581.
2. F. A. Cotton, N. F. Curtis, C. B. Harris, B. F. G. Johnson, S. J. Lippard, J. T. Mague, W. R. Robinson and J. S. Wood, Mononuclear and Polynuclear Chemistry of Rhenium (III): Its Pronounced Homophilicity, *Science*, 1964, **145**, 1305.
3. T. Nguyen, A. D. Sutton, M. Brynda, J. C. Fettinger, G. J. Long and P. P. Power, Synthesis of a Stable Compound with Fivefold Bonding Between Two Chromium(I) Centers, *Science*, 2005, **310**, 844.
4. J. E. McGrady, in *Molecular Metal–Metal Bonds*, ed. S. T. Liddle, Wiley, 2015, ch. 1, pp. 1–22.
5. K. P. Kornecki, J. F. Briones, V. Boyarskikh, F. Fullilove, J. Autschbach, K. E. Schrote, K. M. Lancaster, H. M. L. Davies and J. F. Berry, Direct Spectroscopic Characterization of a Transitory Dirhodium Donor–Acceptor Carbene Complex, *Science*, 2013, **342**, 351.
6. J. R. Prat, C. A. Gaggioli, R. C. Cammarota, E. Bill, L. Gagliardi and C. C. Lu, Bioinspired Nickel Complexes Supported by an Iron Metalloligand, *Inorg. Chem.*, 2020, **59**, 14251–14262.
7. R. C. Cammarota, M. V. Vollmer, J. Xie, J. Ye, J. C. Linehan, S. A. Burgess, A. M. Appel, L. Gagliardi and C. C. Lu, A Bimetallic Nickel–Gallium Complex Catalyzes CO_2 Hydrogenation via the Intermediacy of an Anionic d^{10} Nickel Hydride, *J. Am. Chem. Soc.*, 2017, **139**, 14244–14250.
8. B. Wu, M. J. T. Wilding, S. Kuppaswamy, M. W. Bezpalko, B. M. Foxman and C. M. Thomas, Exploring Trends in Metal–Metal Bonding, Spectroscopic Properties, and Conformational Flexibility in a Series of Heterobimetallic Ti/M and V/M Complexes (M = Fe, Co, Ni, and Cu), *Inorg. Chem.*, 2016, **55**, 12137–12148.
9. J. Coombs, D. Perry, D.-H. Kwon, C. M. Thomas and D. H. Ess, Why Two Metals Are Better Than One for Heterodinuclear Cobalt–Zirconium-Catalyzed Kumada Coupling, *Organometallics*, 2018, **37**, 4195–4203.
10. J. P. Krogman, M. W. Bezpalko, B. M. Foxman and C. M. Thomas, Multi-electron redox processes at a Zr(IV) center facilitated by an appended redox-active cobalt-containing metalloligand, *Dalton Trans.*, 2016, **45**, 11182–11190.
11. J. P. Krogman, B. M. Foxman and C. M. Thomas, Formation and Subsequent Reactivity of a N_2 -Stabilized Cobalt–Hydride Complex, *Organometallics*, 2015, **34**, 3159–3166.
12. Y.-Y. Zhou, D. R. Hartline, T. J. Steiman, P. E. Fanwick and C. Uyeda, Dinuclear Nickel Complexes in Five States of Oxidation Using a Redox-Active Ligand, *Inorg. Chem.*, 2014, **53**, 11770–11777.

13. S. Zhang, P. Cui, T. Liu, Q. Wang, T. J. Longo, L. M. Thierer, B. C. Manor, M. R. Gau, P. J. Carroll, G. C. Papaefthymiou and N. C. Tomson, N–H Bond Formation at a Diiron Bridging Nitride, *Angew. Chem. Int. Ed.*, 2020, **59**, 15215–15219.
14. T. P. Gomba, A. Ramanathan, N. T. Rice and H. S. La Pierre, The chemical and physical properties of tetravalent lanthanides: Pr, Nd, Tb, and Dy, *Dalton Trans.*, 2020, **49**, 15945–15987.
15. N. T. Rice, K. McCabe, J. Bacsa, L. Maron and H. S. La Pierre, Two-Electron Oxidative Atom Transfer at a Homoleptic, Tetravalent Uranium Complex, *J. Am. Chem. Soc.*, 2020, **142**, 7368–7373.
16. N. T. Rice, J. Su, T. P. Gomba, D. R. Russo, J. Telser, L. Palatinus, J. Bacsa, P. Yang, E. R. Batista and H. S. La Pierre, Homoleptic Imidophosphorane Stabilization of Tetravalent Cerium, *Inorg. Chem.*, 2019, **58**, 5289–5304.
17. N. T. Rice, I. A. Popov, D. R. Russo, J. Bacsa, E. R. Batista, P. Yang, J. Telser and H. S. La Pierre, Design, Isolation, and Spectroscopic Analysis of a Tetravalent Terbium Complex, *J. Am. Chem. Soc.*, 2019, **141**, 13222–13233.
18. N. T. Rice, I. A. Popov, D. R. Russo, T. P. Gomba, A. Ramanathan, J. Bacsa, E. R. Batista, P. Yang and H. S. La Pierre, Comparison of tetravalent cerium and terbium ions in a conserved, homoleptic imidophosphorane ligand field, *Chem. Sci.*, 2020, **11**, 6149–6159.
19. A. Sundermann and W. W. Schoeller, Phosphorane–Iminato Complexes of Transition Metals with Heterocubane Structure: A Computational Study, *J. Am. Chem. Soc.*, 2000, **122**, 4729–4734.
20. K. Dehnicke, M. Krieger and W. Massa, Phosphoraneiminato complexes of transition metals, *Coord. Chem. Rev.*, 1999, **182**, 19–65.
21. J. Camacho-Bunquin, M. J. Ferguson and J. M. Stryker, Hydrocarbon-Soluble Nanocatalysts with No Bulk Phase: Coplanar, Two-Coordinate Arrays of the Base Metals, *J. Am. Chem. Soc.*, 2013, **135**, 5537–5540.
22. K. Chakarawet, P. C. Bunting and J. R. Long, Large Anisotropy Barrier in a Tetranuclear Single-Molecule Magnet Featuring Low-Coordinate Cobalt Centers, *J. Am. Chem. Soc.*, 2018, **140**, 2058–2061.
23. K. Chakarawet, M. Atanasov, J. Marbey, P. C. Bunting, F. Neese, S. Hill and J. R. Long, Strong Electronic and Magnetic Coupling in M_4 ($M = Ni, Cu$) Clusters via Direct Orbital Interactions between Low-Coordinate Metal Centers, *J. Am. Chem. Soc.*, 2020, **142**, 19161–19169.
24. S. J. Tereniak and C. C. Lu, in *Molecular Metal-Metal Bonds*, ed. S. T. Liddle, Wiley, 2015, ch. 8, pp. 225–278.
25. C. A. Murillo, An Iron Complex with an Unsupported Fe–Fe Bond, *Angew. Chem. Int. Ed.*, 2009, **48**, 5076–5077.
26. L. Pauling, Metal-metal bond lengths in complexes of transition metals, *Proceedings of the National Academy of Sciences*, 1976, **73**, 4290.
27. M. Konsolakis, Recent Advances on Nitrous Oxide (N_2O) Decomposition over Non-Noble-Metal Oxide Catalysts: Catalytic Performance, Mechanistic Considerations, and Surface Chemistry Aspects, *ACS Catalysis*, 2015, **5**, 6397–6421.
28. A. K. Uriarte, M. A. Rodkin, M. J. Gross, A. S. Kharitonov and G. I. Panov, in *Studies in Surface Science and Catalysis*, eds. R. K. Grasselli, S. T. Oyama, A. M. Gaffney and J. E. Lyons, Elsevier, 1997, vol. 110, pp. 857–864.
29. W. B. Tolman, Binding and Activation of N_2O at Transition-Metal Centers: Recent Mechanistic Insights, *Angew. Chem. Int. Ed.*, 2010, **49**, 1018–1024.
30. K. Severin, Synthetic chemistry with nitrous oxide, *Chem. Soc. Rev.*, 2015, **44**, 6375–6386.
31. S. Yang, W. Zhu, Q. Zhang and Y. Wang, Iron-catalyzed propylene epoxidation by nitrous oxide: Effect of boron on structure and catalytic behavior of alkali metal ion-modified FeOx/SBA-15, *Journal of Catalysis*, 2008, **254**, 251–262.
32. G. Kiefer, L. Jeanbourquin and K. Severin, Oxidative Coupling Reactions of Grignard Reagents with Nitrous Oxide, *Angew. Chem. Int. Ed.*, 2013, **52**, 6302–6305.
33. W. H. Harman and C. J. Chang, N_2O Activation and Oxidation Reactivity from a Non-Heme Iron Pyrrole Platform, *J. Am. Chem. Soc.*, 2007, **129**, 15128–15129.
34. A. Delabie, C. Vinckier, M. Flock and K. Pierloot, Evaluating the Activation Barriers for Transition Metal N_2O Reactions, *The Journal of Physical Chemistry A*, 2001, **105**, 5479–5485.
35. L. Zhao, Y. Wang, W. Guo, H. Shan, X. Lu and T. Yang, Theoretical Investigation of the Fe^+ -Catalyzed Oxidation of Acetylene by N_2O , *The Journal of Physical Chemistry A*, 2008, **112**, 5676–5683.
36. L. Zhou, G. Li, Q.-S. Li, Y. Xie and R. B. King, The diversity of iron–sulfur bonding in binuclear iron carbonyl sulfides, *Canadian Journal of Chemistry*, 2014, **92**, 750–757.
37. P. Mathur, R. S. Ji, A. Raghuvanshi, M. Tauqeer and S. M. Mobin, Cleavage of phosphorus–sulfur bond and formation of $(\mu_4-S)Fe_4$ core from photochemical reactions of $Fe(CO)_5$ with $[(RO)_2PS_2]_2$; ($R = Me, Et, iPr$), *J. Organomet. Chem.*, 2017, **835**, 31–38.
38. R. S. Laitinen and R. Oilunkaniemi, in *Reference Module in Chemistry, Molecular Sciences and Chemical Engineering*, Elsevier, 2019, pp. 1–50.
39. M. Akita, in *Comprehensive Organometallic Chemistry III*, eds. D. M. P. Mingos and R. H. Crabtree, Elsevier, Oxford, 2007, pp. 259–292.
40. A. Müller and E. Diemann, in *Advances in Inorganic Chemistry*, eds. H. J. Emeléus and A. G. Sharpe, Academic Press, 1987, vol. 31, pp. 89–122.
41. M. Shieh, C.-Y. Miu, Y.-Y. Chu and C.-N. Lin, Recent progress in the chemistry of anionic groups 6–8 carbonyl chalcogenide clusters, *Coord. Chem. Rev.*, 2012, **256**, 637–694.
42. H. Ogino, S. Inomata and H. Tobita, Abiological Iron–Sulfur Clusters, *Chem. Rev.*, 1998, **98**, 2093–2122.
43. T. Mitsui, S. Inomata and H. Ogino, Syntheses of closo- $Cp^*_2(CO)_3Fe_2MS_2$ Clusters ($Cp^* = \eta^5-C_5Me_5$; $M = Fe, Ru$) and Molecular Structure of $Cp^*_2(CO)_3Fe_3S_2$, *Inorg. Chem.*, 1994, **33**, 4934–4936.
44. L. C. Roof and J. W. Kolis, New developments in the coordination chemistry of inorganic selenide and telluride ligands, *Chem. Rev.*, 1993, **93**, 1037–1080.
45. M. Reiners, M. Maekawa, C. G. Daniliuc, M. Freytag, P. G. Jones, P. S. White, J. Hohenberger, J. Sutter, K. Meyer, L. Maron and M. D. Walter, Reactivity studies on $[Cp^*Fe(\mu-I)]_2$: nitrido-, sulfido- and diselenide iron complexes derived from pseudohalide activation, *Chem. Sci.*, 2017, **8**, 4108–4122.